*Journal of Chemical Health Risks*

Journal of Chemical Health Risks (2015) 5(1), 45–53

**ORIGINAL ARTICLE**

# Electrochemical Evaluation of Hydroxyapatite/ZrN Coated Magnesium Biodegradable Alloy in Ringer Solution as a Simulated Body Fluid

**Seyed Rahim Kiahosseini[1], Abdollah Afshar[*2], Majid Mojtahedzadeh Larijani[3], Mardali Yousefpour[4]**

[1] Department of Materials Engineering, Science and Research Branch, Islamic Azad University, Tehran, Iran.
[2] Department of Materials Engineering, Sharif University of Technology, Tehran, Iran.
[3] Agriculture Medical and Industrial Research School, Nuclear Science and Technology Research Institute (NSTRI), Karaj, Iran.
[4] Department of Materials Science and Engineering, Semnan University, Semnan, Iran.

*(Received: 22 September 2014 Accepted: 27 November 2014)*

**KEYWORDS**

Biodegradable alloy
Corrosion
Hydroxyapatite
Sputtering

**ABSTRACT:** Magnesium alloys as biodegradable materials can be used in body as an implant materials but since they have poor corrosion resistance, it is required to decrease their corrosion rate by biocompatible coatings. In this study, hydroxyapatite (HA) coatings in the presence of an intermediate layer of ZrN as a biocompatible material, deposited on AZ91 magnesium alloy by ion beam sputtering method at 300 °C temperature and at different times 180, 240, 300, 360 and 420 min. Then changes in corrosion resistance of samples in Ringer's solution as a solution similar to the human body was evaluated in two ways, potentiodynamic polarization and electrochemical impedance spectroscopy (EIS). To investigate the causes of the destruction of the samples, the surface of samples was studied by scanning electron microscopy (SEM). The results showed that because of porous coatings created, the corrosion potential of the samples was about +55mV higher than the uncoated substrate that by changing the deposition time, was not observed the significant change But with increasing deposition time to 360 min, corrosion current decreased which represents an increase of corrosion resistance of magnesium alloy in body solution. However, a further increase in deposition time to 420 min, due to increase thickness and stress in the layer, the corrosion resistance of the samples was reduced. The results of the EIS confirm the corrosion behavior of the polarization method, too.

## INTRODUCTION

Magnesium is lightweight structural metal and Magnesium-base alloys have high strength at about 480 GPa / g / $cm^3$, on the other hands, magnesium and its alloys present a good strength to weight ratio [1, 2].

* Corresponding author: sh_akhlaghi@iaus.ac.ir (H. Akhlaghi).

Magnesium and its alloys are non-toxic to the human body. Magnesium may reduce risk of high blood pressure and heart attacks problems. Release of somewhat $Mg^{+2}$ is required for human body and can be effective in improving bone tissue[3]. The low corrosion resistance of magnesium alloys in human body fluids limits their applications [4, 5]. In addition, calcium phosphate has been noted due to the excellent biocompatibility with human bones. This material has a fast biological reaction and improves the adhesion between bone and implant material and is a suitable abutment for bone growth [6, 7].

The main ingredient of bones and teeth is calcium phosphate called hydroxyapatite (HA) specifically and its composition is $Ca_5 (po_4)_3 OH$ or $Ca_{10} (po_4)_6 (OH)_2$ [8]. HA has a very chemical and crystallographic similarity to mineral composition of natural bone, resulting in to be suitable for dental and medical implant materials [6, 9]. The ideal implant materials are made of this material. However, bulk calcium phosphate is weak and brittle so it is resulting be inappropriate replacement for body parts. For example, high tension is applied to the teeth that will not tolerate. As a result it is better that metallic implant material with good strength, is coated with calcium phosphate [8].

Hydroxyapatite coating improves the corrosion resistance of the implant material [10]. It is well known that properties of deposited films strongly depend on their microstructure such as degree of crystallinity, preferred orientation, grain size, surface roughness and stoichiometry. On the other hand, the film deposition method and parameters can also affect film microstructure [11]. The plasma spray coating method is an economical method for producing HA layer. The experimental result from the application of coatings produced in this way in the body environment, adhesion of the coating is not necessary and due to have amorphous structure is rapidly corroded and degraded[12-14].

Sputtering deposition method was used in this study, in order to create a uniform coating, in addition to increase the wear resistance in presence of an intermediate ZrN layer.

## MATERIALS AND METHODS

The substrates (AZ91 alloy - 10×10×3 $mm^3$) were abraded with 1000, 1200, and 2000 grit silicon carbide papers and were finally mirror polished with 0.03 μm aluminum oxide. Prior to deposition, the specimens were ultrasonically cleaned in both acetone and alcohol bath for 30 min and dried with argon gas. After cleaning, the substrates were immediately inserted into the vacuum chamber on a resistance heater and gradually heated to 573K and 673 for ZrN and HA deposition respectively and the chamber was evacuated to a base pressure of $4\times10^{-3}$ Pa. First, the ZrN films were prepared by ion beam sputtering method on substrates using a Kaufman ion source. The sputtering was initiated by introducing pure Ar (99.999%) and $N_2$ (99.999%) mixed gas at a fixed flow ratio of $\frac{f(N_2)}{f(N_2+Ar)} = 0.5$ into the ion source. The working pressure and the total flow rate of ($Ar+N_2$) mixed gas were kept constant at $8.5\times10^{-3}$ Pa and 20 sccm, respectively. The ZrN film deposition time was 2 hours for each sample. Then the HA films were deposited on the ZrN coating by introducing pure Ar gas at $1.6\times10^{-2}$ Pa working pressure and 20 sccm gas flow rate. The HA deposition times were 180, 240, 300, 360 and 420 min. Ions produced by ion source hit a pure zirconium (99.8%) and pure HA target with 2.8 keV energy and 20 mA current during the sputtering process.

The electrochemical corrosion behavior of the samples was performed by a potentiostat (EG&G model 273) coupled to PC, electrochemical impedance spectroscopy (EIS) and potentiodynamic methods in a ringer solution. The auxiliary and reference electrodes were platinum rod and saturated calomel (SCE) electrode, respectively. The working electrodes were sealed with acrylic resin

and left an area of 0.785 $cm^2$ exposed to the solution during test. The EIS measurements were carried in a frequency range of 100 kHz to 10 mHz with an ac signal of 10 mV amplitude. For polarization test the sample were polarized from −100 mV vs. open circuit potential at a scan rate of 1 mV $s^{-1}$. The ends of scanning were selected after +540 mV vs. open circuit potential. After each experiment the corrosion current ($I_{corr}$) was determined by Tafel plot tradition. For this purpose, the slopes of cathodic and anodic branch were used for extracting the corrosion current. All the presented potentials are as a function of SCE. The surface of corroded samples was characterized by scanning electron microscopy (SEM).

## RESULTS AND DISCUSSION

The results of potentiodynamic polarization tests in ringer solution samples of AZ91 and ZrN / AZ91 and HA / ZrN / AZ91, deposited at different times, are shown in Figure 1. Inactive behavior (Passive) was not visible in the samples.

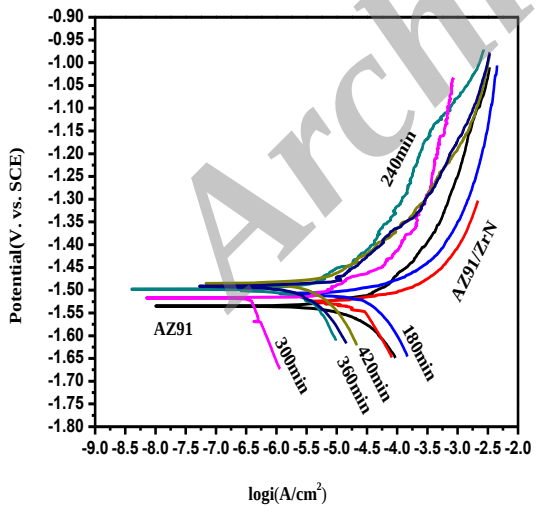


**Figure 1.** Potentiodynamic polarization curves for HA/ZrN/AZ91 samples prepared at 473K and different sputtering time in the ringer solution

The results of the analysis of the polarization curves in Figure 2 show that the corrosion potential of the samples did not show significant changes with increasing deposition time. Potential of HA / ZrN / AZ91 samples are about 55mV more positive than the uncoated substrate, which was very small. These results indicate the presence of micro porosities and crystalline defects in the created coatings. Corrosion potential is a thermodynamic parameter[15, 16]. These results show that the corrosion of samples in the surface of AZ91 substrate occurred too. As a result, small holes and coating defects act as active paths that corrosive solution allowed crossing through them and reach the sub-layer. This has caused the corrosion potential of the coated samples is very close to the corrosion potential of AZ91.

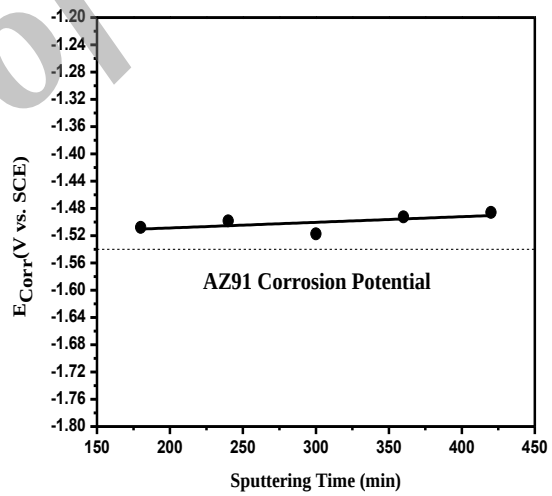


**Figure 2.** The variation of AZ91 corrosion potential coated with HA/ZrN/AZ91 vs sputtering time at 473K

Figure 3 show the current densities of coated samples at different times. The corrosion current density of the samples is reducing with increasing deposition time up to 360 min, which shows the improvement in the corrosion behavior. The corrosion current density of the coated samples for 360 min, approximately is0.33 μA / $cm^2$, about 80 times lower than the corrosion current density of AZ91 and about 40 times less than ZrN /

AZ91. In fact, according to the results of the corrosion potential and the SEM images in Figure 4, about the presence of defects in the layers, the decrease of corrosion current up to 360 min arising from increase in layer thickness and reducing defects such as vacancies in HA layer. At the time of 420 min deposition, corrosion current density increases again due to stresses that affect the coating and consequently formation of micro-cracks in the coating of HA. The cracks act as preferred pathway for ion penetration to substrate surface [17]. Since the corrosion current in the sample is less than ZrN / AZ91, this change in behavior can be attributed to such defects at creation of cracks in the HA coating, so the cracks are visible in the SEM image.

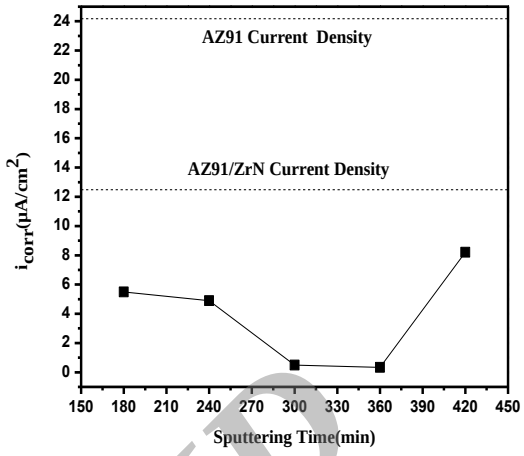


**Figure 3.** The variation of AZ91 corrosion current density coated with HA/ZrN/AZ91 vs sputtering time at 473K

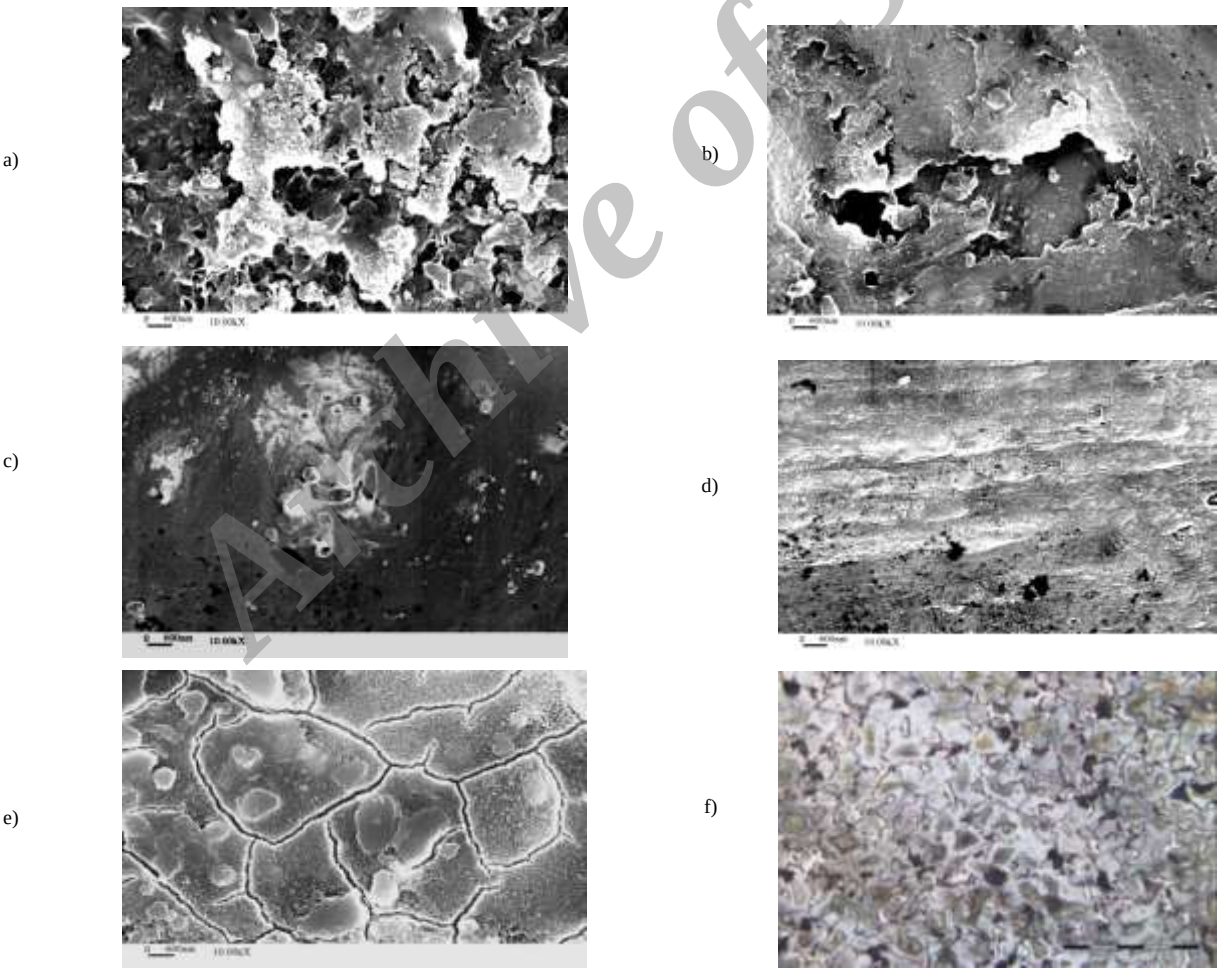


**Figure 4.** Scanning electron microscope images of HA/ZrN/AZ91 samples after corrosion test in ringer solution at different sputtering time, a) 180 min, b) 240 min, c) 300 min, d) 360 min, e) 420 min and f) optical microscope image from AZ91 surface

In Figure 3 and 4, it is observed that the corrosion rate in the sample coated by HA for 180 min is higher than the other samples. In this instance, due to the lack of uniformity of the coating, corrosion has been occurred in areas where coating is the weaker and because of solution penetration from weaker areas to the interface between the coating and the substrate, causing the destruction of the thicker parts too. In other cases, by increasing the thickness and uniformity of the coating, the corrosion rate has been reduced, but in the sample-coated period is 420 min, corrosion has been occurred in preferential pathways. These paths could be micro cracks, grown grain boundaries and paths which affected by internal stresses.

Figure 4 shows optical micrograph of AZ91 gradation after etching in Naytal solution for 5 seconds. Investigations done by ImageJ software showed that the average grain size of AZ91 is about μm40, which is much larger than that, the grain size shown in Figure (4-E) about 4μm. Consequently, the coating made for 420 min, have been attacked by the corrosive solution through grain boundary and preferential pathways and the grain size that observed is related to the grains of coated HA / ZrN. Figure 4-f shows the result of an optical microscopy from substrate surface. The substrate grains are approximately very smaller than grains that shown in Figure 4-e. This results show that, the grains observed in Figure 4-e are HA grains not substrate grains.

The results of electrochemical impedance spectroscopy of samples coated in 300 °C temperature at different times in ringer's solution, has been shown in Figure 5. Nyquist semicircle is clearly visible in these figures. In most curves, three sections of high frequency, low and medium can be observed that each section indicates an interfacial behavior.

At high frequencies, the electrical charge transfer phenomena in double layer formed at the interface between the metal and layer is dominant and at low frequencies is related to the charge transfer within layer[18]. Interfacial behavior in solution is modeled using an equivalent circuit[18].

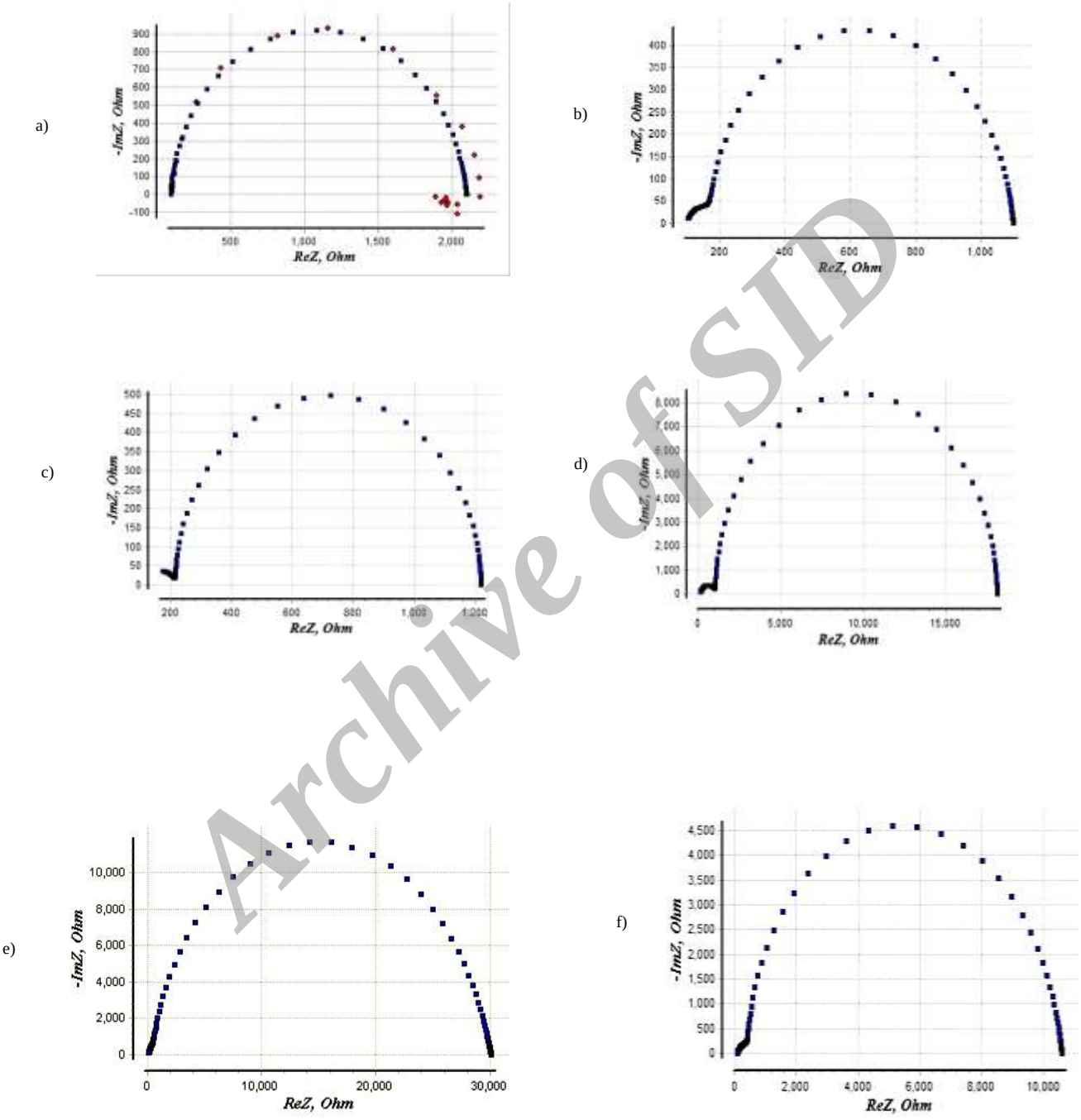


**Figure 5.** Time dependend development of the corrosion resistances (Nypuist plots) of the various HA/ZrN/AZ91 samples in ringer solution, a) 180 min, b) 240 min, c) 300 min, d)360 min and e) 420 min

As shown in Figure 6, in general, the equivalent circuit elements such as capacity, coating (CPE1), the wear resistance ($R_2$), polarization resistance or double layer ($R_3$), double layer capacitance ($C_1$) and the resistance of the solution ($R_1$) is determined to specify performance of coatings in corrosive environment. For example, at high frequencies changes of CPE1 result from the interactions of ions with the coating.

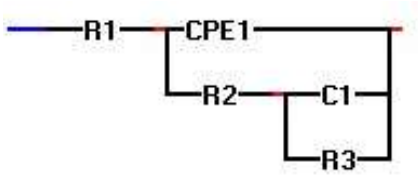


**Figure 6.** Equivalent circuit for EIS analysis

In Figure 6, CPE1 indicates the equivalent capacitor that is created of accumulation of electrical charges on the coating and substrate (both sides of the coating), and coating roles as dielectric. $R_2$ due to the resistance of coating cavities that resist to the transport of attacker ions into the metal. $R_3$ is the charge transfer resistance and the interface of the layer/substrate form a capacitor that its capacity is denoted by $C_1$, and finally, $R_1$ is the resistance, which the solution represents to transport ions to the surface of the sample.

When the samples were coated with HA / ZrN are immersed in Ringer's solution, the less hydrated ions in solution such as $Cl^-$ [19], begins to penetrate the paths of coating porosity. In this case, the impedance of the coating was removed from the ideal behave and behaves as Formula (1) [19]:

$$Z = \frac{1}{Q(j\omega)^n} \qquad (1)$$

In this relation, j is complex number, Q is independent of real constant frequency, ω is the angular frequency and n is Randels power. For the mechanisms under control of penetration n=0.5. According to Table 1, for most of samples investigated in this study n=0.8 was obtained, which shows the penetration mechanism does not definitely exist in corrosion. Moreover, ideal behavior of coating is existed in this mechanism, because ideally is n=1.

$R_1$ indicates the solution resistance. In Table 1, it is observed that resistance is in the range 120-100 $\Omega cm^2$. Created minor changes in solution resistance, possibly due to the weak coating of the sample, which Open circuit corrosion of magnesium causes a change in the concentration of ions and has affected on the resistance of samples. Resistance of solution in most samples is 100 $\Omega cm^2$.

With increasing deposition time until 300 minutes, coating resistance ($R_2$) is about 100 $\Omega cm^2$, which indicates that by increasing the thickness of layer, no changes have been made in resistance of the holes, as the active paths of ion movement. However, the charge transfer resistance ($R_3$) also increased with increasing time of deposition from 900 $\Omega cm^2$ to 1000 $\Omega cm^2$, which has not changed much. These results indicate that increasing the thickness until deposition time of 300 min, has not significant effect on both of the defect coating and charge transfer resistance. Two parameters, layer thickness and density of layer (the amount of compactness) are affected on increasing impedance of the layer [20]. So the amount of defects such as porosity can be affected on the impedance [20]. With increasing deposition time to 360 min, the coating resistance and charge transfer resistance is reached 2000 $\Omega cm^2$ and 28000 $\Omega cm^2$, respectively. Increasing in the wear resistance and charge transfer, lead to increasing in the corrosion resistance. The results of potentiodynamic polarization showed that the sample was coated for 360 min, has maximum corrosion resistance. This behavior is due to increase adhesion to the substrate. Due to appropriate adhesion of layer to the substrate, the presence of ions penetrates to interface of layer/substrate

decreases, thus as can be seen in Table 1, the capacity of double layer for other samples has been decreased from 0.000002 $Fcm^{-2}$ , to the 0.0000002 $Fcm^{-2}$ for sample coated until 360 min.

With increasing deposition time, the coating resistance and the charge transfer resistance decreases to 500 $\Omega cm^2$ and 10000 $\Omega cm^2$ respectively. Then as a result of polarization was also observed, reduced adhesion of layer into substrate due to a large increase in thickness, has been decreased the corrosion resistance or coating resistance and the charge transfer.

**Table 1.** EIS fitted results for spectra obtained from the un-coated and HA/ZrN coated AZ91 magnesium alloy

| Charge Transfer Resistance $R_3(\Omega cm^2)$ | Filme Resistance $R_2$ ($\Omega cm^2$) | Solution Resistance $R_1(\Omega cm^2)$ | Coating Capacitance CPE ($10^{-6}Fcm^{-2}$) / n (dispersion effect of the CPE Components) | Double Layer Constant Phase Element $C_1(10^{-6}Fcm^{-2})$ | Sputtering Time (min) |
|---|---|---|---|---|---|
| **2000** | -- | 100 | -- | 2 | 0(AZ91) |
| **900** | 100 | 100 | 0.8 | 2 | 180 |
| **1000** | 100 | 120 | 0.8 | 2 | 240 |
| **1000** | 100 | 100 | 0.8 | 2 | 300 |
| **28000** | 2000 | 100 | 0.8 | 0.2 | 360 |
| **10000** | 500 | 100 | 0.8 | 2 | 420 |

## CONCLUSION

Adhesion to the substrate improved by mobility of particles and increasing stress relieving and reducing the micro strain on the network. Potential of HA / ZrN / AZ91 samples are about 55mV more positive than the uncoated substrate, which is very small. These results indicate the presence of micro porosities and crystalline defects in the created coatings. The corrosion current density of the coated samples for 360 min, approximately is0.33 μA / $cm^2$, about 80 times lower than the corrosion current density of AZ91 and about 40 times less than ZrN / AZ9. Increasing adhesion until 360 minutes was effective in improving the corrosion behavior, but at more times due to increase in thickness of the layer and the formation of cracks, corrosion resistance decreased. Thus, according to electrochemical impedance spectroscopy test that confirm these results, despite the bilayer coating HA / ZrN can lead to increasing corrosion resistance of biocompatible magnesium alloy in the human body, but increasing time for coating and consequently increasing thickness of layer, is caused to reduce its effectiveness.

## ACKNOWLEDGMENTS

The sample preparation was performed at Nuclear Science and Technology Research Institute (NSTRI). The authors are grateful to Mr. M. Malek for his precious assistance. The authors declare that there is no conflict of interests.

## REFERENCES

1. Altun H., Sinici H., 2008. Corrosion behaviour of magnesium alloys coated with TiN by cathodic arc deposition in NaCl and Na2SO4 solutions. Mater Charact. 59, 266 – 270.

2. Guo-Song W., Ai-Ying W., Ke-Jia D., Cai-Yun X., Wei D., Ai-Jiao X., 2008. Fabrication of Cr coating on

AZ31 magnesium alloy by magnetron sputtering. Trans of Nonferrous Met Soc of China. 18, 329-333.

3. Wen C., Guan S., Peng L., Ren C., Wang X., Hu Z., 2009. Characterization and degradation behavior of AZ31 alloy surface modified by bone-like hydroxyapatite for implant applications. Applied Surface Science. 255, 6433–6438.

4. Wen C., Guan S., Peng L., Ren C., Wang X., Hu Z., 2009. Characterization and degradation behavior of AZ31 alloy surface modified by bone-like hydroxyapatite for implant applications. Appl Surf Sci. 255, 6433–6438.

5. Altun H., Sen S., 2005. The effect of DC magnetron sputtering AlN coatings on the corrosion behaviour of magnesium alloys. Surf Coat Technol. 197, 193– 200.

6. Li H., Li Z.X., Li H., Wu Y.Z., Wei Q., 2009. Characterization of plasma sprayed hydroxyapatite/$ZrO_2$ graded coating. Materials and Design. 30, 3920–3924.

7. Yuan Q., Golden T. D., 2009. Electrochemical study of hydroxyapatite coatings on stainless steel substrates. Thin Solid Films. 518, 55–60.

8. Leo´n B., Jansen A., eds., Thin Calcium Phosphate Coatings for Medical Implants. Springer. New York, 2009.

9. Yousefpour M., Afshar A., Yang X., Li X., Yang B., Wu Y., Chen J., Zhang X., 2006. Nano-crystalline growth of electrochemically deposited apatite coating on pure titanium. J Electroanal Chem. 589, 96–105.

10. Yan Z.C., Cheng Z.R., Long L.C., Cheng G.J., 2010. Comparison of calsium phosphate coating on Mg-Al and Mg-Ca alloy and their corrosion behavior in Hank's solution. Surf Coat Technol. 24, 3636-3640.

11. Jiménez H., Restrepo E., Devia A., 2006. Effect of the substrate temperature in ZrN coatings grown by the pulsed arc technique studied by XRD. Surf Coat Technol. 201, 1594–1601.

12. Javidi M., Javadpour S., Bahrololoom M.E., Ma J., 2008. Electrophoretic deposition of natural hydroxyapatite on medical grade 316L stainless steel. Mat Sci Engin. 28, 1509-1515.

13. Socola G., Macoveib A. M., Miroiua F., Stefana N., Dutaa L., Dorciomana G., Mihailescua I.N., Petrescub S.M., Stanc G.E., Marcovc D.A., Chiriacd A., Poeata I., 2010. Hydroxyapatite thin films synthesized by pulsed laser deposition and magnetron sputtering on PMMA substrates for medical applications. Mat Sci Engin B. 169, 159–168.

14. Song L., Gan L., Xiao Y.F., Wu Y., Wu F., Gu Z.W., 2011. Antibacterial hydroxyapatite/chitosan complex coatings with superior osteoblastic cell response. Materials Letters. 65, 974–977.

15. Huang J.H., Ouyang F.Y., Yu G.P., 2007. Effect of film thickness and Ti interlayer on the structure and properties of nanocrystalline TiN thin films on AISI D2 steel. Surf Coat Technol. 201, 7043–7053.

16. Chou W.J., Yu G.P., Huang J.H., 2001. Corrosion behavior of TiN-coated 304 stainless steel. Corrosion Science. 43, 2023-2035.

17. Sun W., Nesic S., presented in part at the NACE InternationalCORROSION CONFERENCE AND EXPO. 2007, USA, 2007.

18. Jamesh M., Kumar S., Narayanan T.S.N.S., 2012. Electrodeposition of hydroxyapatite coating on magnesium for biomedical applications. J Coatings Technol Res. 9(4), 495–502.

19. Rout T.K., 2007. Electrochemical impedance spectroscopy study on multi-layered coated steel sheets. Corrosion Science. 49, 794–817.

20. Roland T., Pelletier H., Krier J., 2013. Scratch resistance and electrochemical corrosion behavior of hydroxyapatite coatings on Ti6Al4V in simulated physiological media. J Appl Electrochem. 43, 53–63.